

Test case	Cfr. vs. [14] (flat-top)	Cfr. vs. [12] (cosecant)	Cfr. vs. [7] (flat-top)	Cfr. vs. [7] (cosecant)	Cfr. vs. [10] (cosecant)
W (Number of equivalent solutions)	512	32	16	32	32
ϵ (Fitting precision inside τ_2 region)	2×10^{-2}	17×10^{-2}	5×10^{-3}	17×10^{-2}	22×10^{-2}
τ_2 (Fitting region)	$ \sin\alpha \leq 0.37$	$-0.05 \leq \sin\alpha \leq 0.85$	$ \sin\alpha \leq 0.31$	$0 \leq \sin\alpha \leq 0.83$	$-0.18 \leq \sin\alpha \leq 0.59$
L/λ (Size)	11.68	7.28	6.80	6.93	7.53
ψ/λ (Minimum elements spacing)	0.40	0.48	0.46	0.51	0.55
S (Final elements number)	13	11	10	12	12
Elements number saving vs. best case available in literature	58%	15%	9%	8%	8%

Tab. I. Simulation parameters adopted for the test cases concerning one-dimensional arrays.

Notably, by virtue of the extremely low computational burden of the overall design algorithm, each example required less than 15 seconds to be generated by a calculator having an Intel Core i7-3537U 2.50GHz CPU and a 10 GB RAM.

Finally, it is worth noting that, although the proposed procedure can manage any element factor in the synthesis, all the following power-pattern figures just refer to the square-amplitude distribution of the array factors.

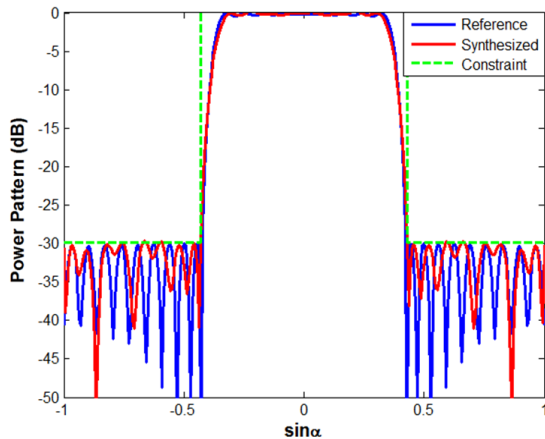


Fig. 2. Reference (blue curve, from [14]) and synthesized (red curve) power pattern in the test case of Susection IV.1. Exploited upper-bound constraint (green curve) is also depicted. Simulation parameters: $d/\lambda=0.5$; $Q=29$; $N=201$; $v=0.05$; $\sigma/\lambda=0.1$; $\eta/\beta=0.025$.

IV.1 Comparison with [14] (flat-top beam)

We adopted as reference the power pattern depicted in blue color in Fig. 2, which has been synthesized in [14] by means of a 31-elements sparse array. This flat-top field guarantees a ripple equal to 0.4455 dB for $-20^\circ \leq \alpha \leq 20^\circ$, and fulfills an upper-bound constraint (depicted in green color in Fig. 2) of -30 dB for $-90^\circ \leq \alpha \leq -25^\circ$ and $25^\circ \leq \alpha \leq 90^\circ$. By factorizing this power pattern, we have been able to determine 512 equivalent field solutions. Then, we have selected amongst them the one corresponding to the excitation distribution having the minimum ℓ_1 norm and, by applying to the latter the proposed

approach, we identified a 13-elements sparse array able to radiate the power-pattern distribution depicted in red color in Fig. 2. As it can be seen, the synthesized solution results equivalent, in terms of radiation performance, to the reference one. Therefore, the proposed procedure has allowed, with respect to the best solution shown in [14], a 58% elements saving without experiencing any power-pattern worsening. The synthesized sparse array's excitation amplitudes and phases are respectively depicted in figures 3 and 4.

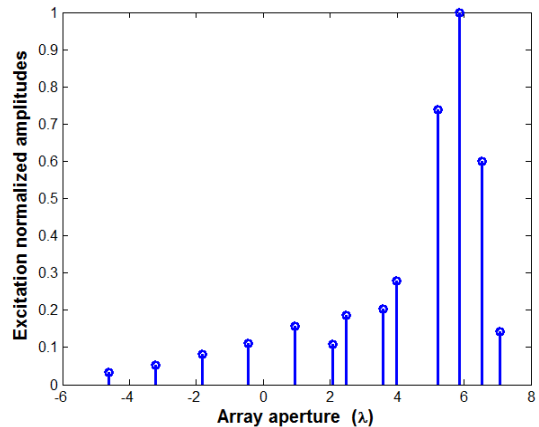


Fig. 3. Excitation amplitudes of the maximally-sparse array radiating the red pattern of Fig. 2.

IV.2 Comparison with [12] (cosecant beam)

We used as reference square-amplitude array factor the power pattern depicted in blue color in Fig. 5. In [12], the FBMPM allowed generating it through a sparse array composed by 13 elements located over an aperture of 7.5λ . By exploiting the proposed approach, we have been able to generate the power pattern depicted in red color in Fig. 9 by exploiting a sparse array composed by 11 elements located over an aperture of 7.4λ . Therefore, without experiencing any loss in terms of radiation performance, and exploiting a practically equivalent aperture size, we reduced of the 15.4%

the elements number achieved in [12]. The amplitude and phase distributions of the synthesized array excitations are shown in figures 6 and 7, respectively.

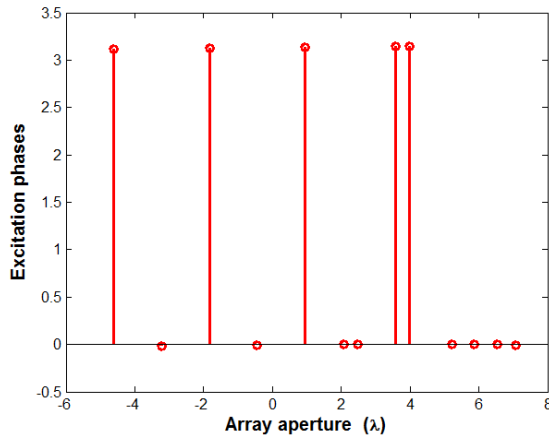


Fig. 4. Excitation phases of the maximally-sparse array radiating the red pattern of Fig. 2.

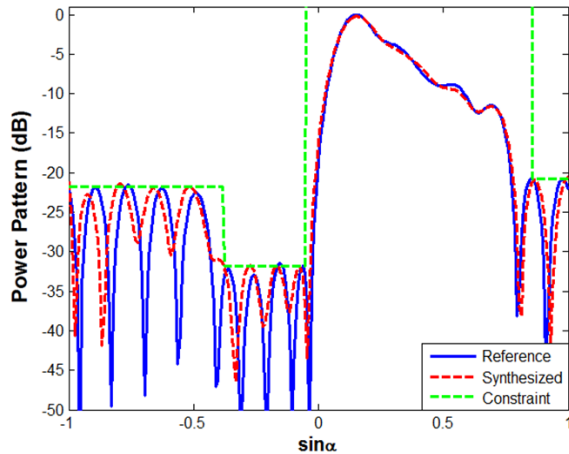


Fig. 5. Adopted upper bound (green curve) and reference (blue curve, from [12]) and synthesized (red curve) power patterns for the second test case. Simulation parameters: $d/\lambda=0.5$; $Q=16$; $N=321$; $\nu=0.005$; $\sigma/\lambda=0.025$; $\eta/\beta=0.05$.

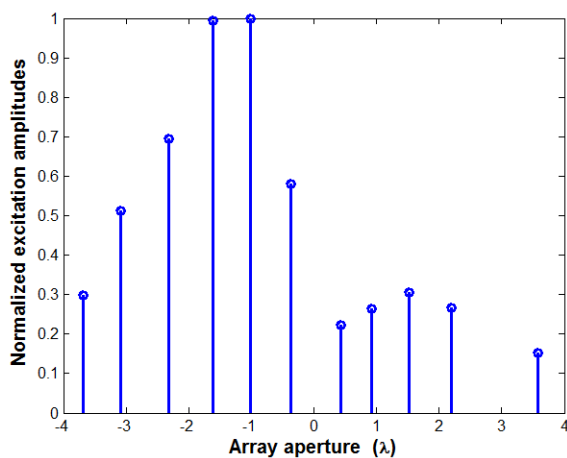


Fig. 6. Excitation amplitudes of the maximally-sparse array radiating the red pattern of Fig. 5.

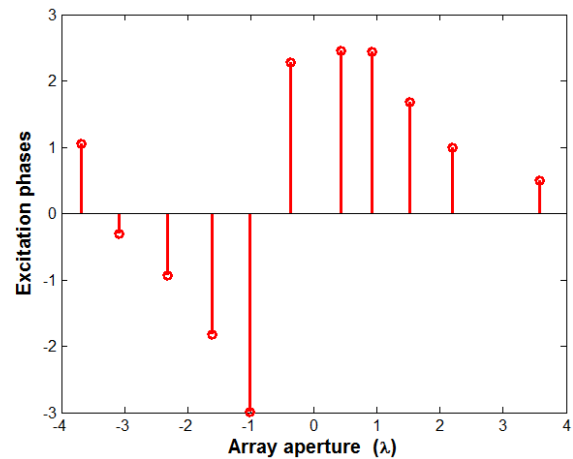


Fig. 7. Excitation phases of the maximally-sparse array radiating the red pattern of Fig. 5.

IV.3 Comparison with [7] (flat-top beam)

In the third test case, we used as reference power pattern the flat-top beam depicted in blue color in Fig. 8, which has a maximum ripple of ± 0.58 dB, a peak sidelobe level of -35.6 dB with respect to the maximum power pattern value for $|\alpha| \geq 27.5^\circ$. In [7], BCS has been effectively exploited to generate it through a sparse array composed by 11 elements located over an aperture of 7λ . Also, this power pattern has been generated in [12] by exploiting the FBMPM and using 10 radiating elements.

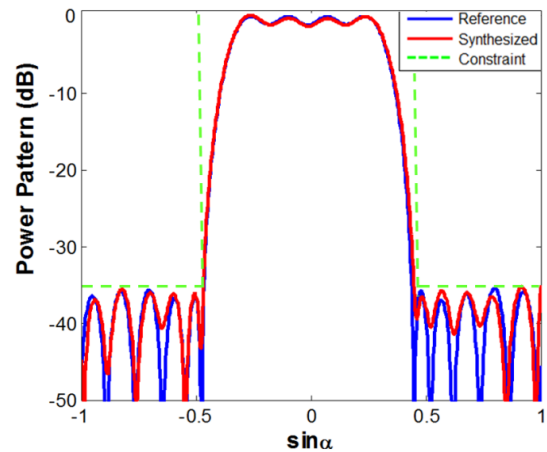


Fig. 8. Third test case: adopted upper bound (green curve); reference (blue curve, from [7]) and synthesized (red curve) power patterns. Simulation parameters: $d/\lambda=0.5$; $Q=15$; $N=38$; $\nu=0.04$; $\sigma/\lambda=0.19$; $\eta/\beta=0.09$.

As first design operation, we have generated this power pattern without changing any parameter with respect to [7] (see Table 1). Then, we have factorized the resulting polynomial and applied our CS-based routine to all the equivalent far-field distributions corresponding to it, with the aim of assessing the effectiveness of the adoption of (7). In particular, in each instance we have analyzed the ℓ_1 norm of the excitation set of the reference array factor and counted the active elements of the sparse array coming out from the CS routine. The outcomes of such experiments have been

summarized in Fig. 9. As it can be seen, the excitation set having the minimum ℓ_1 norm is also the one that leads to the minimum number of active elements in the array designed through CS. This circumstance (which has been also verified in the previous and following test cases) confirms the arguments in Section III.1 about the capability of identifying in a simple fashion the far-field distribution which more easily lends itself to a CS-based ‘sparsification’ process.

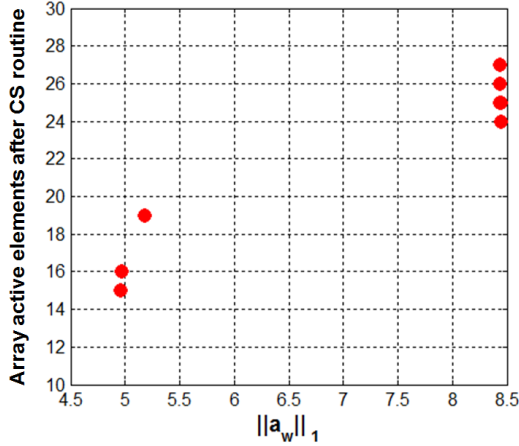


Fig. 9. Concerning the impact on the CS performance of the ℓ_1 norm of the excitations of the different solutions coming out from the statement of the reference power pattern.

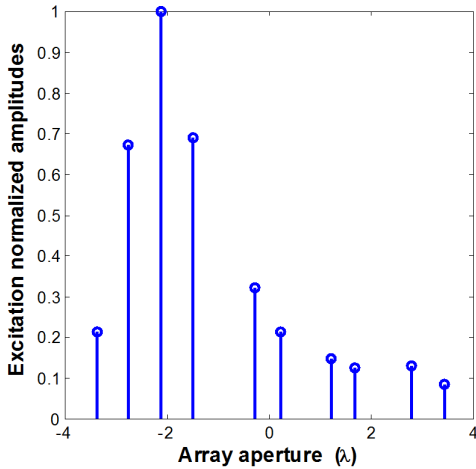


Fig. 10. Excitation amplitudes corresponding to the red pattern of Fig. 8.

By applying the post-processing procedure to the array layout having the minimum number of elements at the end of the CS routine, we have achieved a radiation performance which favorably compares to [7] through a sparse array composed by 10 elements located over an aperture of 6.8λ with a minimum spacing of 0.46λ .

The achieved array locations and excitations are depicted in Fig. 10 (amplitude distribution) and Fig. 11 (phase distribution), respectively, while Fig. 8 shows the exploited upper-bound function and a superposition of the reference and synthesized square-amplitude array factors. As it can be seen, the achieved power pattern perfectly fits the reference one.

Notably, in this test case the results achieved by means of the proposed strategy are equivalent to those one reported in [12], while they turn out being improved with respect to [7] in all terms of number of elements, dimensions and performances. Finally, we highlight the important circumstance that the execution of the third step of the procedure allowed us to reduce N of about the 50% with respect to the case wherein just the first two steps of the approach are exploited.

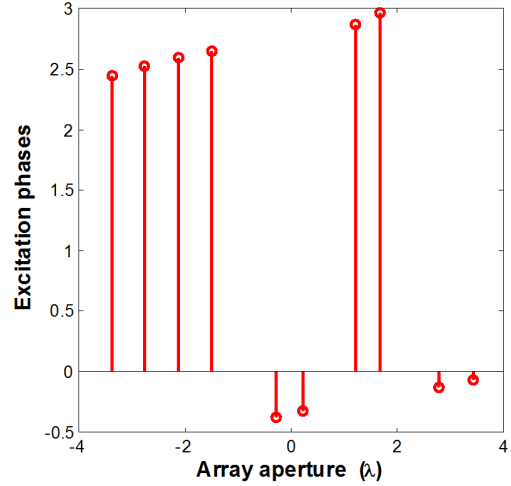


Fig. 11. Excitation phases corresponding to the red pattern of Fig. 8.

IV.4 Comparison with [7] (cosecant beam)

We adopted as reference power pattern the square-cosecant field shown in blue color in Fig. 12. In [7], by adopting BCS this pattern has been synthesized through a sparse array composed by 13 elements located over an aperture of 7.5λ . By exploiting the proposed approach, we have been able to reduce again the array’s number of elements and size, respectively, without any radiation-performance loss.

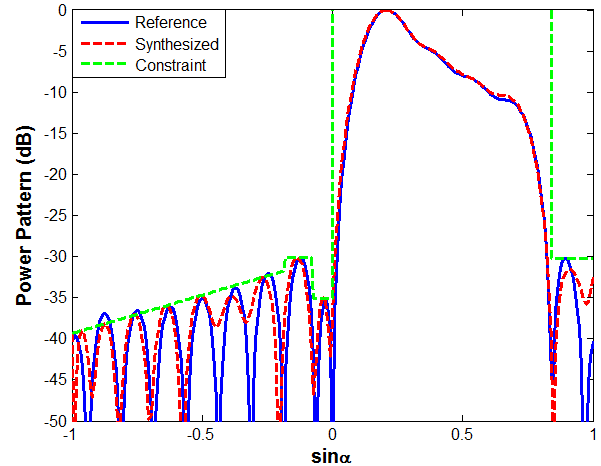


Fig. 12. Synthesis of a maximally-sparse array radiating a square-cosecant pattern with a specific sidelobes decay. Reference (blue curve, from [7]) and synthesized (red curve) square-amplitude array factors. Adopted upper bound (green curve) also depicted. Simulation parameters: $d/\lambda=0.5$; $Q=16$; $N=161$; $v=0.03$; $\sigma/\lambda=0.05$; $\eta/\beta=0.01$.

This circumstance is shown in Fig. 12, wherein a comparison between reference and synthesized patterns is reported. The designed array is composed by 12 elements located over an aperture of 6.9λ with a minimum spacing of 0.51λ . The corresponding excitation amplitudes and phases are depicted in figures 13 and 14, respectively.

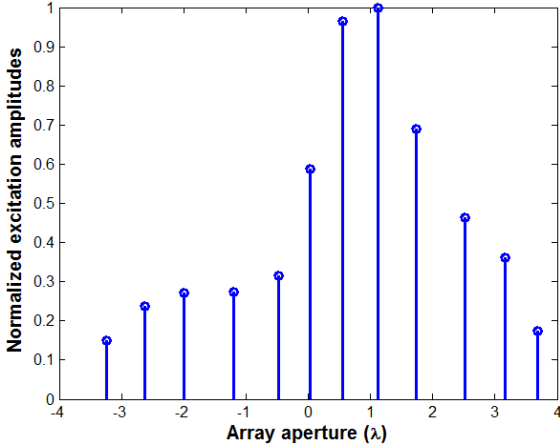


Fig. 13. Excitation amplitudes of the maximally-sparse array radiating the red pattern of Fig. 12.

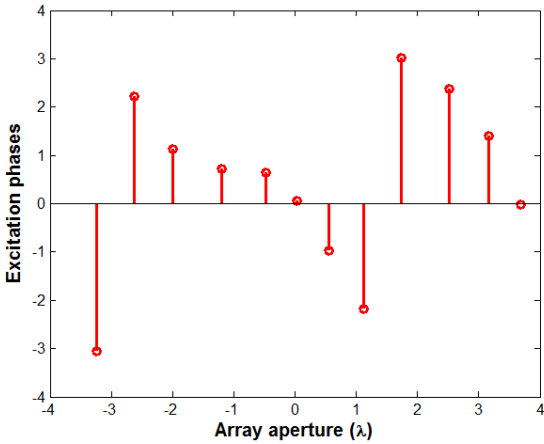


Fig. 14. Excitation phases of the maximally-sparse array radiating the red pattern of Fig. 12.

IV.5 Comparison with [10] (cosecant beam)

In the fifth test case, we aimed at synthesizing the square-cosecant power pattern depicted in blue color in Fig. 15. In [10], CS has been exploited to generate it by means of a sparse array composed by 13 elements located over an aperture of 8λ . Notably, by means of the presented approach, we have achieved an equivalent radiation performance while reducing both the elements number and the aperture size. In particular, the synthesized sparse array is composed by 12 elements located over an aperture of 7.5λ with a minimum spacing of 0.56λ .

The achieved antenna layout and excitations are depicted in Fig. 16 (amplitude distribution) and Fig. 17 (phase distribution), respectively. A superposition of the reference and synthesized patterns is shown in Fig. 15, wherein it can be noticed that all the design goals and constraints have been fulfilled. The same figure shows the upper-bound function

exploited to bind the sidelobes as desired, which also points out the flexibility of the overall synthesis procedure.

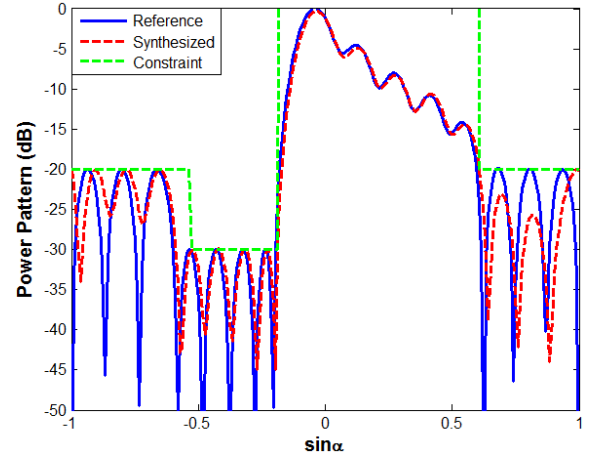


Fig. 15. Synthesis of a maximally-sparse array radiating a square-cosecant pattern with a non-uniform, piecewise-constant sidelobe level behavior. Adopted upper bound (green curve); reference (blue curve, from [10]) and synthesized (red curve) square-amplitude array factors. Simulation parameters: $d/\lambda=0.5$; $Q=16$; $N=161$; $v=0.005$; $\sigma/\lambda=0.05$; $\eta/\beta=0.08$.

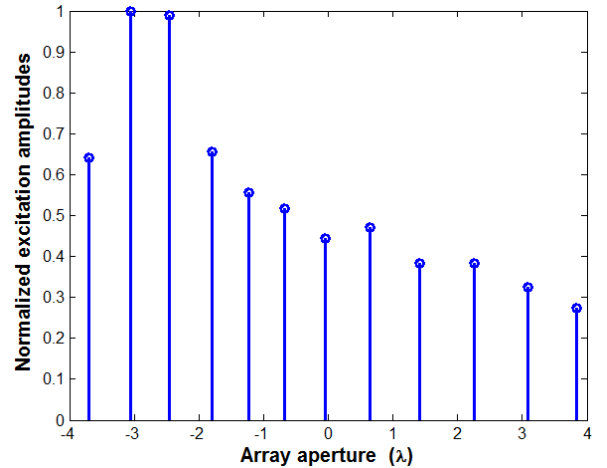


Fig. 16. Array excitation amplitudes corresponding to red pattern of Fig. 15.

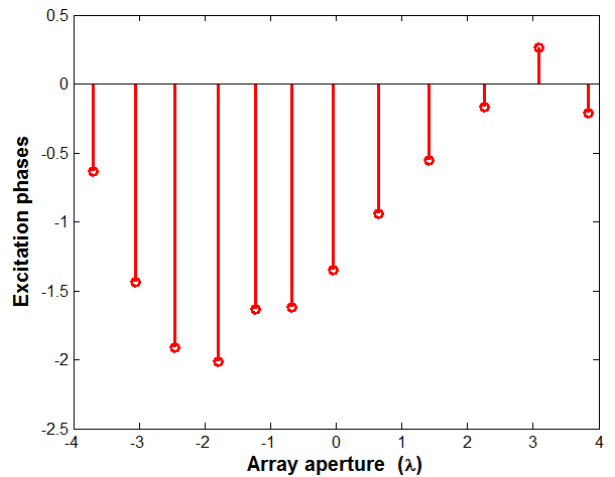


Fig. 17. Array excitation phases corresponding to the red pattern of Fig. 15.

IV.6 Synthesis of a factorable beam through a planar array

As a final test case, we show the outcomes of a numerical experiment concerning a simple way to extend the proposed procedure to the synthesis of planar sparse arrays with factorable patterns.

Coming to details, we aimed at synthesizing a beam having a flat-top behavior along the azimuth angle and a square-cosecant behavior along the elevation angle, which is of interest in radar applications as well as for radio-base stations. In so doing, we took as a reference the pattern generated from the factorization of the fields depicted in blue color in figures 8 and 12, respectively. Notably, exploitation of the results in [7] would require $13 \times 11 = 143$ elements to generate the desired radiation pattern. On the other side, a straightforward application of our results in Subsections IV.3 and IV.4 already reduces to $12 \times 10 = 120$ the number of required elements. This circumstance is coherent with the fact that, as long as a pattern is factorable, the elements number reduction in the planar array is roughly doubled with respect to the one experienced in the two underlying one-dimensional arrays.

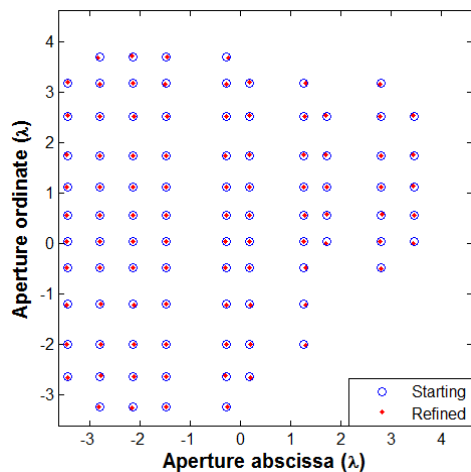


Fig. 18. Array layout achieved by factorizing the one-dimensional solutions shown in Subsections IV.3 and IV.4 and discarding those elements having a normalized excitation amplitude lower than 0.04: elements' location before (blue circles) and after (red dots) running the final 'refinement' algorithm.

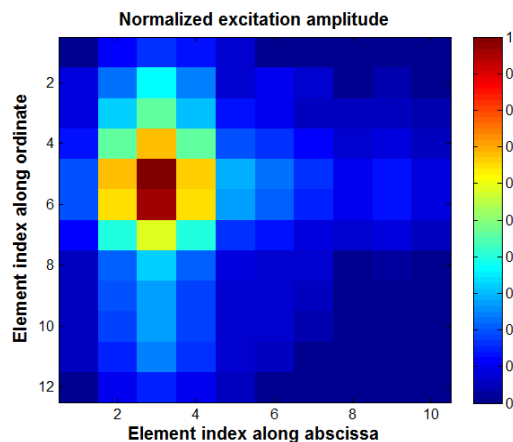


Fig. 19. Normalized excitation amplitudes associated to the refined layout shown in Fig. 18.

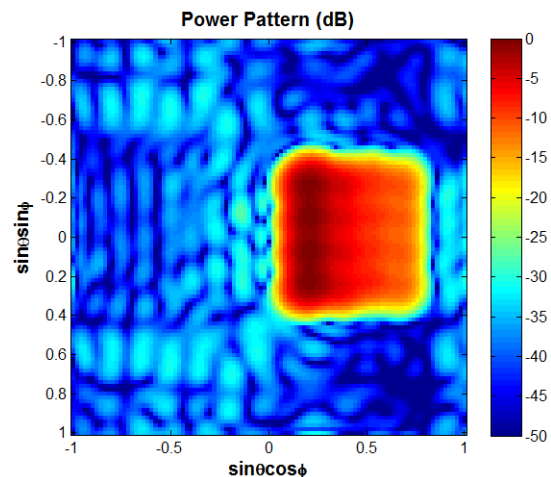


Fig. 20. Power pattern of the planar array having the refined layout of Fig. 18 and the excitations whose amplitude distribution is shown in Fig. 19.

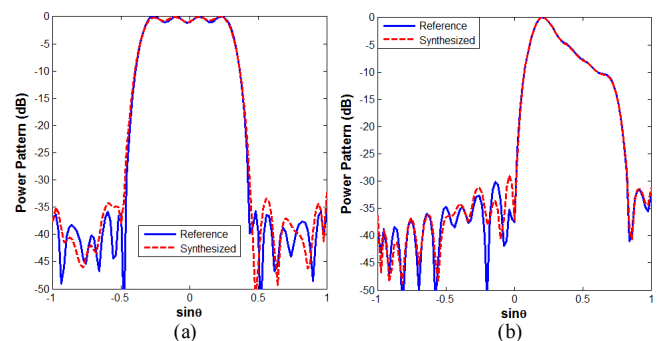


Fig. 21. Main cuts along ordinate [subplot (a)] and abscissa [subplot (b)] of the power pattern shown in Fig. 20: reference (blue color) and synthesized (red color) solutions.

Interestingly, a simple application of the third step of the proposed procedure, i.e., of the techniques presented in Subsection III.3, allows a further considerable reduction of elements. In fact, by simply 'eliminating' those elements having an excitation amplitude lower than $v=0.04$ we achieved the array layout depicted in Fig. 18 (blue circles), which is composed by 94 elements. Then, by adapting to the two-dimensional layouts case the approach in (10),(11), in such a way to *jointly* refine *both* the x and y array locations, we finally achieved the layout depicted in Fig. 18 (red dots), and the corresponding optimal excitations depicted in Fig. 19 (just amplitude is shown). The achieved power pattern is shown in figures 20 (in the two-dimensional spectral plane) and 21 (along its two main cuts), wherein θ and ϕ respectively represent the elevation and azimuth angles. As it can be seen, a very good agreement is achieved between the reference field and the main cuts of the synthesized pattern.

Notably, the overall approach allows to save roughly the 58% of the elements with respect to a fully populated array with a uniform $\lambda/2$ spacing, and roughly the 34% of elements (tolerating a slight worsening of the very low sidelobe levels) with respect to a simple factorization of the solutions in [7].

IV. CONCLUSIONS

We have introduced and tested a new approach, inspired from CS, for the synthesis of shaped beams by means of linear

arrays having the minimum possible number of elements. The presented technique takes maximum advantage from the multiplicity of different far field and source distributions (having different amounts of sparsity) corresponding to a fixed power pattern, and also from the circumstance that different power patterns may equally fulfill the initial constraints.

These features, as well as the use of a reduced cardinality of the tentative array, has allowed us to improve the amount of sparsity of the synthesized array in a number of benchmark problems present in the state-of-the-art literature. In particular, different methods based on LP [14], FBMPM [12], CS [10] and BCS [7] have been considered for comparison. In all cases, the proposed approach always performed equally or better than the considered techniques.

The procedure can be easily extended to other cases of interest in several applications, including the design of arrays with factorable patterns (see Section IV.6) as well as one-dimensional simply reconfigurable arrays (by exploiting the ideas in [36]).

REFERENCES

- [1] M. I. Skolnik, "Chapter 6. Nonuniform Arrays," in *Antenna Theory, Part I*, R. E. Collin and F. Zucker (eds), New York, McGraw-Hill, 1969.
- [2] R. E. Willey, "Space tapering of linear and planar arrays," *IRE Trans. on Antennas and Propagation*, vol. 10, n. 4, pp. 369-377, 1962.
- [3] T. A. Milligan, "Space-tapered circular (ring) array," *IEEE Antennas and Propagation Magazine*, vol. 46, n. 3, pp. 70-73, 2004.
- [4] O. M. Bucci, M. D'Urso, T. Isernia, P. Angeletti, and G. Toso, "Deterministic synthesis of uniform amplitude sparse arrays via new density taper techniques," *IEEE Transactions on Antennas and Propagation*, vol. 58, n. 6, pp. 1949-1958, 2010.
- [5] O. M. Bucci, T. Isernia, and A. F. Morabito, "An effective deterministic procedure for the synthesis of shaped beams by means of uniform-amplitude linear sparse arrays," *IEEE Transactions on Antennas and Propagation*, vol. 61, n. 1, pp. 169-175, 2013.
- [6] G. Oliveri and A. Massa, "Bayesian compressive sampling for pattern synthesis with maximally sparse non-uniform linear arrays," *IEEE Transactions on Antennas and Propagation*, vol. 59, n. 2, pp. 467-481, 2011.
- [7] G. Oliveri, M. Carlin, and A. Massa, "Complex-weight sparse linear array synthesis by Bayesian Compressive Sampling," *IEEE Transactions on Antennas and Propagation*, vol. 60, n. 5, pp. 2309-2326, 2012.
- [8] G. Prisco and M. D'Urso, "Maximally sparse arrays via sequential convex optimizations," *IEEE Antennas and Wireless Propagation Letters*, vol. 11, pp. 192-195, 2012.
- [9] W. Zhang, L. Li, and F. Li, "Reducing the number of elements in linear and planar antenna arrays with sparseness constrained optimization," *IEEE Transactions on Antennas and Propagation*, vol. 59, n. 8, pp. 3106-3111, 2011.
- [10] B. Fuchs, "Synthesis of sparse arrays with focused or shaped beam pattern via sequential convex optimizations," *IEEE Transactions on Antennas and Propagation*, vol. 60, n. 7, pp. 3499-3503, 2012.
- [11] Y. Liu, Z. Nie, and Q. H. Liu, "Reducing the number of elements in a linear antenna array by the matrix pencil method," *IEEE Transactions on Antennas and Propagation*, vol. 56, n. 9, pp. 2955-2962, 2008.
- [12] Y. Liu, Q. H. Liu, and Z. Nie, "Reducing the number of elements in the synthesis of shaped-beam patterns by the forward-backward matrix pencil method," *IEEE Transactions on Antennas and Propagation*, vol. 58, n. 2, pp. 604-608, 2010.
- [13] Y. Liu, Q. H. Liu, and Z. Nie, "Reducing the number of elements in multiple-pattern linear arrays by the extended matrix pencil methods," *IEEE Trans. on Antennas Propag.*, vol. 62, n. 2, pp. 652-660, 2014.
- [14] S. E. Nai, W. Ser, Z. L. Yu, and H. Chen, "Beampattern synthesis for linear and planar arrays with antenna selection by convex optimization," *IEEE Transactions on Antennas and Propagation*, vol. 58, n. 12, pp. 3923-3930, 2010.
- [15] A. Trucco and V. Murino, "Stochastic optimization of linear sparse arrays," *IEEE Journal of Oceanic Engineering*, vol. 24, n. 3, pp. 291-299, 1999.
- [16] D. Caratelli and M. C. Viganò, "A novel deterministic synthesis technique for constrained sparse array design problem," *IEEE Transactions on Antennas and Propagation*, vol. 59, n. 11, pp. 4085-4093, 2011.
- [17] D. Caratelli and M. C. Viganò, "Analytical synthesis technique for linear uniform-amplitude sparse arrays," *Radio Science*, vol. 46, n. 4, 2011.
- [18] A. K. Bhattacharyya, "Projection matrix method for shaped beam synthesis in phased arrays and reflectors," *IEEE Transactions on Antennas and Propagation*, vol. 55 n. 3, pp. 675-683, 2007.
- [19] A. F. Morabito, T. Isernia, and L. Di Donato, "Optimal synthesis of phase-only reconfigurable linear sparse arrays having uniform-amplitude excitations," *Progress In Electromagnetics Research*, vol. 124, pp. 405-423, 2012.
- [20] A.K. Bhattacharyya, *Phased Array Antennas: Floquet Analysis, Synthesis, BFNs, and Active Array Systems*, Chapter 11, "Shaped-Beam Array Design: Optimization Algorithms," pp. 357-374, Wiley, 2006.
- [21] T. Isernia, O. M. Bucci, and N. Fiorentino, "Shaped beam antenna synthesis problems: feasibility criteria and new strategies," *Journal of Electromagnetic Waves and Applications*, vol. 12, pp. 103-137, 1998.
- [22] E. J. Candès, J. K. Romberg, and T. Tao, "Robust uncertainty principles: exact signal reconstruction from highly incomplete frequency information," *IEEE Transactions on Information Theory*, vol. 52, n. 2, pp. 489-509, 2006.
- [23] E. J. Candès and M. B. Wakin, "An Introduction To Compressive Sampling," *IEEE Signal Processing Magazine*, vol. 25, pp. 21-30, March 2008.
- [24] E. J. Candès, M. Wakin, and S. Boyd, "Enhancing sparsity by L_1 reweighted minimization," *Journal of Fourier Analysis and Applications*, vol. 14, n. 5, pp. 877-905, 2008.
- [25] O. M. Bucci, G. Franceschetti, "On the degrees of freedom of scattered fields," *IEEE Transactions on Antennas and Propagation*, vol. AP-37, pp. 918-926, 1989.
- [26] P. M. Woodward and J. D. Lawson, "The theoretical precision with which an arbitrary radiation-pattern may be obtained from a source of finite size," *Journal of the Institution of Electrical Engineers - Part III: Radio and Communication Engineering*, vol. 95, n. 37, pp. 363-370, 1948.
- [27] O. M. Bucci, G. D'Elia, G. Mazzarella, and G. Panariello, "Antenna pattern synthesis: a new general approach," *Proceedings of the IEEE*, vol. 82, n. 3, pp. 358-371, 1994.
- [28] L. Manica, N. Anselmi, P. Rocca, and A. Massa, "Robust mask-constrained linear array synthesis through an interval-based particle SWARM optimization," *IET Microw. Antennas Propag.*, vol. 7, n. 12, pp. 976-984, 2013.
- [29] A. Pirhadi, M. H. Rahmani, and Alireza Mallahzadeh, "Shaped beam array synthesis using particle swarm optimisation method with mutual coupling compensation and wideband feeding network," *IET Microw. Antennas Propag.*, vol. 8, n. 8, pp. 549-555, 2014.
- [30] G. W. Wasilkowski, "On average complexity of global optimization problems," *Mathematical Programming*, vol. 57, n. 1-3, pp. 313-324, 1992.
- [31] O. M. Bucci, T. Isernia, A. F. Morabito, "Optimal synthesis of circularly symmetric shaped beams," *IEEE Transactions on Antennas and Propagation*, vol. 62, n. 4, pp. 1954-1964, 2014.
- [32] S. G. Mallat and Z. Zhang, "Matching pursuits with time-frequency dictionaries," *IEEE Transactions on Signal Processing*, vol. 41, n. 12, pp. 3397-3415, 1993.
- [33] T. Blumensath and M. E. Davies, "Iterative thresholding for sparse approximations," *Journal of Fourier Analysis and Applications*, vol. 14, n. 5, 2008.
- [34] S. Chen, D. Donoho D., and D. Saunders D., "Atomic decomposition by basis pursuit," *SIAM Journal on Scientific Computing*, vol. 20, n. 1, pp. 33-61, 1999.
- [35] R. Tibshirani, "Regression shrinkage and selection via the lasso," *Journal of the Royal Statistical Society: Series B*, vol 58, no.1, pp.267-288, 1996.
- [36] A. F. Morabito, A. Massa, P. Rocca, and T. Isernia, "An effective approach to the synthesis of phase-only reconfigurable linear arrays," *IEEE Transactions on Antennas and Propagation*, vol. 60, n. 8, pp. 3622-3631, 2012.